Exploration of nonlinearly shunted piezoelectrics as vibration absorbers

B Zhou[1,2], C Zang[1], X Wang[1]

[1]Nanjing University of Aeronautics and Astronautics, Jiangsu Province Key Laboratory of Aerospace Power System, Nanjing 210016, China
[2]Collaborative Innovation Center of Advanced Aero-engine, Nanjing 210016, China

E-mail: biao.zhou@nuaa.edu.cn

Abstract. Practical realization of a nonlinearly shunted piezoelectric vibration absorber is numerically explored in this research. It is widely known that the linear resonant piezoelectric shunting strategy, acting as a tuned mass damper, is limited by the massive inductance required in low-frequency cases and sensitivity to drifts in structural frequencies. In order to overcome this limitation, a nonlinear piezoelectric shunting strategy is proposed based on the nonlinear energy sink theory. The essential idea is to passively absorb vibrational energy from the host structure through the intentional use of nonlinearity in piezoelectric shunting. The nonlinearly shunted piezoelectrics are supposed to work over a broad frequency band with a smaller inductance requirement compared with the linear resonant shunting. The nonlinearly shunted piezoelectric vibration absorber is built and applied in a cantilevered beam. Major challenges coming from the nonlinear tuning design for an effective vibration absorber exempted from high isolated response curves will be covered in this research. This numerical study is supposed to pave the way for experimental investigations that are currently in process.

1. Introduction

The piezoelectric shunt damping technique has received sustaining attentions for the purpose of vibration suppression in recent decades. It exploits the capability of piezoelectric materials attached onto vibrational structures to transform mechanical (strain) energy into electrical energy, which is then dissipated in the electrical circuit. In a piezoelectric shunted structure, this conversion capability highly depends on: 1) the ability to absorber the strain energy of the structure into the piezoelectric material; 2) the capability of the piezoelectric materials to transform this strain energy into electrical energy. The former depends on the distribution of modal strain energy in the structure, which requires that piezoelectric materials should be located in the proper zone; The latter is determined by the electric shunting design, which generally aims to maximize the energy dissipation.

The classic resonant shunt circuit has been completely investigated by Hagood and Von Flotow since 1990 [1]. It exhibits the advantage of simplicity, compactness and high efficiency when properly tuned with respect to a certain modal frequency of the structure in the way analogous to the linear tuned mass damper. while at the same time, the use of resonant shunt circuits is limited by the massive inductance required in low-frequency cases and sensitivity to drifts in both structural frequencies and optimal electric parameters.

A nonlinear piezoelectric shunting strategy has been proposed in order to improve the damping performance in early research efforts [2]. The essential idea is formed in the framework of Nonlinear Energy Sink (NES) theory [3], which is characterized by essential (strong) nonlinearity. In NES devices, essential nonlinearity can be achieved by a number of structure configurations, such as sophisticated wire-based rigs [4], visco-elastic membrane [5], vibro-impact attachments [6], specially shaped tracks [7] and elastomeric bumpers [8]. The NES can carry out targeted energy transfer, i.e. an irreversible channelling of vibrational energy from the host structure to the absorber. This sort of absorber has been developed for various applications including shock/seismic mitigation [9], aeroelastic instability suppression [10] and acoustic mitigation [5], etc.

An attempt is undertaken to construct a prototype of a piezoelectric-based NES through shunting the piezoelectric materials by a so-called essentially nonlinear shunt circuit [11]. Nonlinearity can be readily achieved by proper circuit design in piezoelectric shunting. It is reported that the intentional introduction of nonlinearity into a resonant shunt circuit might significantly alters the global dynamics of the resultant piezo-mechanical system. In particular, when the structure undergoes harmonic forcing, the nonlinear shunt circuit can resonantly interact with the primary system in a broadband manner. Despite this appealing benefit, complex dynamical phenomena might arise as by-product due to the presence of essential nonlinearity. For instance, quasi-periodic regimes of motion and detached resonance curves are usually encountered in the nonlinear forced response. These potential adverse effects are always of major concern for real NES designs [12, 13, 14]. Unfortunately, the energy-dependent nonlinear dynamics of the piezo-mechanical system under harmonic excitation remains elusive, which may undermine the practical applicability of the nonlinearly shunted piezoelectric vibration absorber.

The principal purpose of this research is to conduct an in-depth study of the aforementioned piezoelectric-based NES as an effective vibration absorber. The nonlinearly shunted piezoelectric vibration absorber is built and applied in a cantilevered beam. The rich dynamics of the linear mechanical structure coupled with a nonlinear shunted piezoelectric attachment is numerically investigated. To this end, an efficient modeling of the piezo-mechanical system based on a finite element description and a modal reduction are presented in Sec. 2; the global dynamics of the resulting integrated system is fully examined in Sec. 3 and special attention is paid to the nonlinear forced response when the cantilevered beam is excited by a mono-harmonic forcing; conclusions are drawn in the end.

2. Modeling of mechanical structures with piezoelectrics

In this section, the shunted piezoelectric's interaction with the mechanical structure is modeled. The classic resonant shunt circuit will be briefly revisited. The derivation of resonant shunt circuit will also benefit the non-dimensionalization of the following nonlinear shunt circuit. The adopted modeling methodology in this research is a general finite element description with a modal reduction put forward by M Neubauer and J Wallaschek [15].

2.1. Finite element description

Each node of a piezoelectric element has an extra electric degree of freedom (electrical potential). For a general structure with piezoelectric materials, the discretized coupled piezoelectric and structural field equations are given in term of nodal displacement $\mathbf{u}$ and nodal electrical potential $\mathbf{v}$ in commercial finite element programs as:

$$\begin{bmatrix} \mathbf{M}_{\mathrm{mm}} & \mathbf{0} \\ \mathbf{0} & \mathbf{0} \end{bmatrix} \begin{bmatrix} \ddot{\mathbf{u}} \\ \ddot{\mathbf{v}} \end{bmatrix} + \begin{bmatrix} \mathbf{K}_{\mathrm{mm}} & \mathbf{K}_{\mathrm{me}} \\ \mathbf{K}_{\mathrm{me}}^{\mathrm{T}} & \mathbf{K}_{\mathrm{ee}} \end{bmatrix} \begin{bmatrix} \mathbf{u} \\ \mathbf{v} \end{bmatrix} = \begin{bmatrix} \mathbf{f}_{\mathrm{ext}} \\ \mathbf{q} \end{bmatrix} \tag{1}$$

where $\mathbf{M}_{\mathrm{mm}}$ and $\mathbf{K}_{\mathrm{mm}}$ are the global mass matrix and stiffness matrix of the integrated piezo-mechanical system, respectively; piezoelectric coupling matrix $\mathbf{K}_{\mathrm{me}}$ couples the structural degrees of freedom (dofs) and electric dofs; $\mathbf{K}_{\mathrm{ee}}$ relates the electric charge $\mathbf{q}$ and electrical potential $\mathbf{v}$ at each node; the external force is given by $\mathbf{f}_{\mathrm{ext}}$.

Condensation of electric dofs is then performed due to the presence of electrodes. Internal electric dofs inside piezoelectric materials can be statically condensed since internal electric charges are null. All the nodes on each electrode surface can be coupled together to define a unique master electrical dof as a result of the equipotential physical constraint. Two electric dofs are accordingly left for each piezoceramic covered by a pair of electrodes with charges denoted by $+q_{\mathrm{p}}$ and $-q_{\mathrm{p}}$, respectively. One electrode is grounded (zero electrical potential) so that the attached electric dof can be neglected. Electrical potential of the remaining electrode is v_{p}.

Subsequently, the mechanical subsystem can be transformed into modal coordinates $\mathbf{z}$ with mass-normalized eigenvectors $\mathbf{\Phi}$. They are derived by solving the eigenvalue problem in the case of short-circuit electrodes ($v_{\mathrm{p}} = 0$) so that:

$$\mathbf{\Phi}^{\mathrm{T}}\mathbf{M}_{\mathrm{mm}}\mathbf{\Phi} = \mathbf{I}, \quad \mathbf{\Phi}^{\mathrm{T}}\mathbf{K}_{\mathrm{mm}}\mathbf{\Phi} = \mathbf{\Lambda} = \mathrm{diag}(\omega_{\mathrm{sc},i}^2), \quad i = 1, 2, \cdots \tag{2}$$

$\mathbf{\Phi}$ may consist of a reduced set of eigenvectors, which implies a modal truncation. $\mathbf{\Lambda}$ is a diagonal matrix so that the structural dofs are decoupled. After a static condensation of electric dofs and modal truncation, Eq. (1) reads

$$\begin{bmatrix} \mathbf{I} & \mathbf{0} \\ \mathbf{0} & \mathbf{0} \end{bmatrix} \begin{bmatrix} \ddot{\mathbf{z}} \\ \ddot{\mathbf{v}}_{\mathrm{p}} \end{bmatrix} + \begin{bmatrix} \mathbf{\Lambda} & \kappa \\ \kappa^{\mathrm{T}} & -\mathbf{C}_{\mathrm{p}} \end{bmatrix} \begin{bmatrix} \mathbf{z} \\ \mathbf{v}_{\mathrm{p}} \end{bmatrix} = \begin{bmatrix} \mathbf{f}_{\mathrm{mod}} \\ -\mathbf{q}_{\mathrm{p}} \end{bmatrix}, \quad \kappa = \mathbf{\Phi}^{\mathrm{T}}\mathbf{K}_{\mathrm{me}}, \quad \mathbf{f}_{\mathrm{mod}} = \mathbf{\Phi}^{\mathrm{T}}\mathbf{f}_{\mathrm{ext}} \tag{3}$$

where $\mathbf{C}_{\mathrm{p}}$ is also a diagonal matrix of the capacitance of the individual piezoceramics; the modal coupling matrix κ relates the generalized mechanical modal dofs with the electric dof, namely, the electrical voltage across distributed electrodes $\mathbf{v}_{\mathrm{p}}$.

When the electrodes are isolated, the electric charge load vector $\mathbf{q}_{\mathrm{p}}$ becomes null. With $\mathbf{v}_{\mathrm{p}} = \mathbf{C}_{\mathrm{p}}^{-1}\kappa^{\mathrm{T}}\mathbf{z}$ extracted from the second relation, Eq. (3) reduces to

$$\ddot{\mathbf{z}} + \mathbf{\Lambda}_{\mathrm{iso}} = \mathbf{0} \quad with \quad \mathbf{\Lambda}_{\mathrm{iso}} = \mathbf{\Lambda} + \kappa\mathbf{C}_{\mathrm{p}}^{-1}\kappa^{\mathrm{T}} \tag{4}$$

Diagonal elements of $\mathbf{\Lambda}_{\mathrm{iso}}$ typically give good approximations of the natural frequencies in the case of isolated electrodes, i.e., $\omega_{\mathrm{iso}}^2 \approx \omega_{\mathrm{sc}}^2 + \mathrm{diag}(\kappa\mathbf{C}_{\mathrm{p}}^{-1}\kappa^{\mathrm{T}})$. Their deviations from short circuit frequencies indicate the piezoelectric coupling strength. A generalized Electro-Mechanical Coupling Coefficient (EMCC) [16] is therefore defined for the i-th structural mode:

$$K_i^2 = \frac{\omega_{\mathrm{iso},i}^2 - \omega_{\mathrm{sc},i}^2}{\omega_{\mathrm{iso},i}^2} \approx \frac{\kappa_i^2}{\omega_{\mathrm{sc},i}^2 C_{\mathrm{p}} + \kappa_i^2} \tag{5}$$

In essence, the EMCC is a measure of the effectiveness of piezoceramics to convert mechanical strain energy into electrical energy and vice versa. It can be calculated by means of finite element analysis or measured experimentally. Modal reduction is a very useful technique to tackle large size finite element models. Next, the configuration of a nonlinear piezoelectric shunt circuit will be described.

2.2. Nonlinear shunt circuit

Before proceeding into the construction of a nonlinear shunt circuit, the classic resonant shunt circuit will be preliminarily revisited. When an inductance L and resistance R are connected in series with the electrodes of piezoceramics (see Fig. 1(a)), the governing equation of the resonant shunt circuit is expressed as:

$$L\ddot{q}_{\mathrm{p}} + R\dot{q}_{\mathrm{p}} + v_{\mathrm{p}} = 0 \tag{6}$$

For simplicity and conciseness, only a single piezoceramic is considered and the system dynamics in the vicinity of a specified i-th structural mode is examined. Substituting Eq. (6) into Eq. (3) yields:

$$\begin{bmatrix} 1 & 0 \\ 0 & L \end{bmatrix} \begin{bmatrix} \ddot{z} \\ \ddot{q}_\mathrm{p} \end{bmatrix} + \begin{bmatrix} \gamma\omega_\mathrm{sc}^2 & 0 \\ 0 & R \end{bmatrix} \begin{bmatrix} \dot{z} \\ \dot{q}_\mathrm{p} \end{bmatrix} + \begin{bmatrix} \omega_\mathrm{sc}^2 + \frac{\kappa^2}{C_\mathrm{p}} & \frac{\kappa}{C_\mathrm{p}} \\ \frac{\kappa}{C_\mathrm{p}} & \frac{1}{C_\mathrm{p}} \end{bmatrix} \begin{bmatrix} z \\ q_\mathrm{p} \end{bmatrix} = \begin{bmatrix} f_\mathrm{mod} \\ 0 \end{bmatrix} \tag{7}$$

where $\gamma\omega_\mathrm{sc}^2$ accounts for structural damping.

This resonant circuit allows attenuation of resonance vibration through proper tuning of the electric parameters in the way analogous to a mechanical tuned mass damper. The tuned resonant shunt circuit with optimal parameters L_res and R_res will be hereafter chosen as a reference system for the construction of a nonlinear shunt circuit.

$$L_\mathrm{res} = \frac{1}{\omega_\mathrm{iso}^2 C_\mathrm{p}}, \quad R_\mathrm{res} = \frac{\sqrt{2}K}{\omega_\mathrm{iso}^2 C_\mathrm{p}} \tag{8}$$

2.2.1. Configuration of the nonlinear shunt circuit

The nonlinear shunt circuit is characterized by intensional nonlinearity, which can be realized by introducing a ferroelectric capacitance made of (Hf, Zr)-doped barium titanate ceramics, as denoted by C_nl in Fig. 1(b). A physical description of the nonlinear voltage-charge characteristic of the ferroelectric capacitance can be obtained as [17]:

$$v_c(q) = \frac{1}{C_0} q + \alpha q^3 \tag{9}$$

where C_0 is the linearized capacitance near $q = 0$.

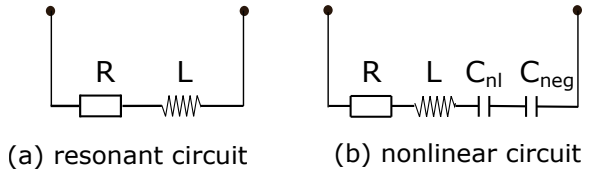

Figure 1. Piezoelectric shunt circuits

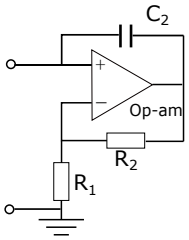

Figure 2. Negative capacitance $C_\mathrm{neg} = -\frac{R_1}{R_2} C_2$

The requirement of essential nonlinearity also implies that the stiffness terms should be non-linearizable. Hence, a negative capacitance C_neg (see Fig. 2) is introduced into the nonlinear circuit in Fig. 1(b); if not, the presence of the inherent capacitance of the piezoceramic C_p will undermine the realization of essential nonlinearity. The negative capacitance needs an operational amplifier to form a negative-impedance converter circuit with little power consumption (see Fig. 2).

A combination of the inherent piezoelectric capacitance C_p, the linearized term C_0 of the ferroelectric capacitance and the negative capacitance C_neg in series results in the residual capacitance C_res, with $1/C_\mathrm{res} = \delta_\mathrm{res}/C_p$. One can also express the inductance L and resistance R in the nonlinear shunt circuit in terms of optimal parameters $(L_\mathrm{res}; R_\mathrm{res})$ for the resonant circuit as $\varepsilon L_\mathrm{res}$ and βR_res, respectively. The governing equation reads in this case:

$$\begin{bmatrix} 1 & 0 \\ 0 & \varepsilon L_\mathrm{res} \end{bmatrix} \begin{bmatrix} \ddot{z} \\ \ddot{q}_\mathrm{p} \end{bmatrix} + \begin{bmatrix} \gamma\omega_\mathrm{sc}^2 & 0 \\ 0 & \beta R_\mathrm{res} \end{bmatrix} \begin{bmatrix} \dot{z} \\ \dot{q}_\mathrm{p} \end{bmatrix} + \begin{bmatrix} \omega_\mathrm{sc}^2 + \frac{\kappa^2}{C_\mathrm{p}} & \frac{\kappa}{C_\mathrm{p}} \\ \frac{\kappa}{C_\mathrm{p}} & \frac{\delta_\mathrm{res}}{C_\mathrm{p}} \end{bmatrix} \begin{bmatrix} z \\ q_\mathrm{p} \end{bmatrix} + \begin{bmatrix} 0 \\ \alpha q_\mathrm{p}^3 \end{bmatrix} = \begin{bmatrix} f_\mathrm{mod} \\ 0 \end{bmatrix} \tag{10}$$

It is noted that the item $\frac{\delta_{\text{res}}}{C_{\text{p}}} q_{\text{p}}$ is still retained in the second relation of Eq. (10). This linear term, usually unavoidable, always appears in reality. Nevertheless, it is negligible as long as it is many orders of magnitude smaller than the cubic term and it would not affect performance of a NES device [4]. The equations of the piezoelectric structure will be subsequently developed in a dimensionless form suitable for nonlinear analysis.

2.2.2. Dimensionless form of equations of motion

Determination of the order of magnitude of the nonlinear capacitance is of practical significance for the nonlinear shunt circuit design. This issue can be simplified by defining a critical nonlinear coefficient α_{cr} so that $\frac{q_{\text{p,max}}}{C_{\text{p}}} = \alpha_{\text{cr}} q_{\text{p,max}}^3$, where $q_{\text{p,max}}$ is the maximum electric charges exhibited in Eq. (7) for the resonant circuit with optimal parameters $(L_{\text{res}}; R_{\text{res}})$. Consequently the actual nonlinear coefficient α can be measured by α_{cr} as $\alpha = \theta \alpha_{\text{cr}}$.

The parameter $q_{\max}$ also helps to rescale physical quantities. By using the relations in Eq. (5) and Eq. (8), Eq. (10) can be rewritten in the dimensionless form as:

$$\begin{bmatrix} 1 & 0 \\ 0 & \varepsilon \end{bmatrix} \begin{bmatrix} x'' \\ q'' \end{bmatrix} + \begin{bmatrix} \lambda & 0 \\ 0 & \beta\sqrt{2}K \end{bmatrix} \begin{bmatrix} x' \\ q' \end{bmatrix} + \begin{bmatrix} 1 & K \\ K & \delta_{\text{res}} \end{bmatrix} \begin{bmatrix} x \\ q \end{bmatrix} + \begin{bmatrix} 0 \\ \theta \frac{\kappa^2}{K^2} q^3 \end{bmatrix} = \begin{bmatrix} f \\ 0 \end{bmatrix} \tag{11}$$

where the dimensionless quantities are defined as:

$$z = q_{\max} x, \quad q_{\text{p}} = \frac{q_{\max}}{\sqrt{L_{\text{res}}}} q, \quad f_{\text{mod}} = q_{\max} \omega_{\text{iso}}^2 f, \quad \lambda = \frac{\gamma \omega_{\text{sc}}^2}{\omega_{\text{iso}}} \tag{12}$$

Differentiations in Eq. (11) are with respect to the eigentime $\tau = \omega_{\text{iso}} t$. In this dimensionless form, system matrices largely depend on the generalized electro-mechanical coupling coefficient K for the specified structural mode. Apparently, The parameter set $(\varepsilon = 1, \beta = 1, \delta_{\text{res}} = 1, \theta = 0)$ corresponds to the tuned resonant circuit. It is reported that a grounded NES configuration featured by: a) strong mass asymmetry between the primary subsystem and nonlinear subsystem; b) essential stiffness nonlinearity [3]. The nonlinear shunt circuit is constructed to reproduce the dynamics of a unground mechanical NES by setting essential nonlinearity (i.e. $\delta_{\text{res}} \ll 1$) and small inductance (i.e. $\varepsilon < 1$). The dimensionless form of equations of motion is suitable for nonlinear analysis. In an effort to understand the dynamics of this coupled electromechanical system, electrical parameters of the nonlinear shunt circuit will be further discussed in the following numerical studies.

3. Dynamics of the nonlinearly shunted piezo-mechanical system

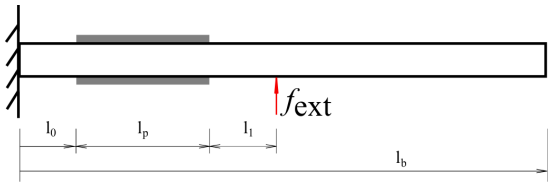

Figure 3. Representation of a cantilevered beam with bonded piezoceramics

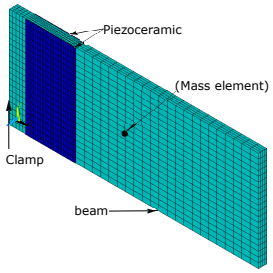

Figure 4. FE model of the piezo-mechanical system

The nonlinearly shunted piezoelectric vibration absorber is built and applied in a cantilevered aluminium beam, as sketched in Fig. 3. Two identical C-82 PZT patches (manufactured by

FUJI Ceramics Co.) are perfectly glued on the top and bottom surface near the clamp in order to enhance the energy conversion. Geometry and material properties of the beam and piezoceramics are provided in Table 1. Both patches are polarized along the same thickness direction. Deformation of piezoelectric patches along with bending movement of the beam will thus create opposite electric field directions due to their relative location. The finite element model discretized by SOLID 185 (for the beam) and SOLID 5 (for piezoceramics) in Ansys is presented in Fig. 4. All electric dofs on each electrode are condensed into a unique master dof. The electric dofs on the electrode surfaces bonded to the beam are grounded.

Table 1. Geometry and material properties of the beam and piezoceramics.

Description	Value	Description	Value
Beam		Piezoceramics	
Mass density	2800 Kg/m^3	Mass density	7500 Kg/m^3
Young's modulus	72 Gpa	Young's modulus E_{11}	62 Gpa
Length l_b	150 mm	Young's modulus E_{33}	51 Gpa
width	60 mm	Length l_p	30 mm
Thickness	5 mm	width	60 mm
Damping coefficient γ	0.004	Thickness	0.3 mm
Position l_0	20 mm	Piezoelectric constant d_{31}	-266 pm/V
Position l_1	15 mm	Permittivity ε_{11}^S	13.94 nF/m
		Permittivity ε_{33}^S	12.97 nF/m

Focus is then concentrated on the 1st bending mode of the clamped beam with a short circuit natural frequency $\omega_{\text{sc}} = 212.72\,\text{Hz}$. After a modal reduction, electromechanical parameters of the resonant circuit tuned for 1$^{\text{st}}$ bending mode are summarized in Table 2. It is stated that the resonant shunt circuit with optimal parameters $(L_{\text{res}}; R_{\text{res}})$ is taken as a reference system. The nonlinear shunt circuit can be therefore constructed in the manner presented in Sec. 2.2. Rich dynamics of the linear mechanical structure coupled with a nonlinear shunted piezoelectric attachment will be numerically investigated. First, special attention is paid to the harmonic balance method since it is employed as a main numerical tool in this research.

Table 2. Electromechanical parameters of the resonant circuit tuned for 1$^{\text{st}}$ bending mode.

Description	Value	Description	Value
Tot. capacitance	155.76 nF	Natural Freq. ω_{iso}	213.59 Hz
EMCC. $K(\%)$	9.02	Resistance R_{res}	610.5 Ω
Coupling term κ	0.0478	Inductance L_{res}	3.5645 H
Natural Freq. ω_{sc}	212.72 Hz		

3.1. Numerical tool: harmonic balance method

The harmonic balance method (HBM) is a computationally efficient alternative to time marching method for nonlinear structural analyses when the response is periodic in time [18, 19]. Rewrite

Eq. 11 in the compact matrix form and denote $\mathbf{y} = [x, q]^{\mathrm{T}}$:

$$\mathbf{M}\mathbf{y}'' + \mathbf{D}\mathbf{y}' + \mathbf{K}\mathbf{y} + \mathbf{f}_{\mathrm{nl}}(\mathbf{y}) = \mathbf{f} \tag{13}$$

where $\mathbf{f}$ represents the external periodic excitation with a single fundamental frequency ω. The harmonic balance method proceeds by first substituting a temporal Fourier series expansion of the solution variables into the governing equations. In other words, the periodic solution $\mathbf{y}$ is sought of the form:

$$\mathbf{y}(t) = \mathbf{Y}^0 + \sum_{k=1}^{N_h} \mathbf{Y}^{ck}\cos(k\omega t) + \mathbf{Y}^{sk}\sin(k\omega t) \tag{14}$$

where N_h is the number of retained harmonics. Inserting the periodic solution into Eq. 13 yields a set of $2 \times (2N_h + 1)$ nonlinear algebraic equations $G(\mathbf{Y}, \omega) = \mathbf{0}$ for $2 \times (2N_h + 1)$ unknowns $\mathbf{Y} = [\mathbf{Y}^0, \mathbf{Y}^{c1}, \mathbf{Y}^{s1}, \cdots, \mathbf{Y}^{ck}, \mathbf{Y}^{sk}, \cdots]^T$. The problem of searching for a periodic solution to the nonlinear dynamic system Eq. (13) therefore boils down to finding zeros of an algebraic function.

Provided that a starting point $(\mathbf{Y}^0, \omega^0)$ is found by directly solving $G(\mathbf{Y}^0, \omega^0) = \mathbf{0}$ at a frequency point where the nonlinear effect is not dominant, this system is going to be subsequently solved by an arc length continuation. Continuation allows numerically finding a series of points $(\mathbf{Y}^j, \omega^j)$ along a solution branch, which meet the convergence criterion $G(\mathbf{Y}^j, \omega^j) = \mathbf{0}$. A predictor-corrector and adaptive step control scheme [20] has been adopted to enhance and speed up the path-following process in order to search periodic solutions over a range of values for ω. Stability of periodic solutions is determined by the Floquet theory in this research. Further details about the continuation and Floquet theory can be found in Ref. [21].

3.2. Nonlinear normal modes

As it is known, dynamics of the free vibration of the coupled nonlinear system is governed by the topological structure and bifurcations of nonlinear normal modes (NNM) [3]. NNMs are universally defined as not necessarily synchronous periodic motions of the undamped and unforced nonlinear system. A number of different numerical methods are developed for calculations of NNMs [22]. Stemming from linear normal modes at low magnitude, NNMs of the non-dissipative autonomous system ($\mathbf{D} = \mathbf{0}, \mathbf{f} = \mathbf{0}$) are computed by means of the harmonic balance method combined with the arc-length continuation presented in this research. Nonlinear shunt circuit parameters are given as ($\varepsilon = 0.1, \beta = 1, \delta_{\mathrm{res}} = 0.01, \theta = 0.1$). Only *cosine* terms are retained with $N_h = 5$ in the approximation of $\mathbf{y}$ in Eq. 14. This is deduced from a phase condition in which the initial velocity $\mathbf{y}'(0)$ are set to zero.

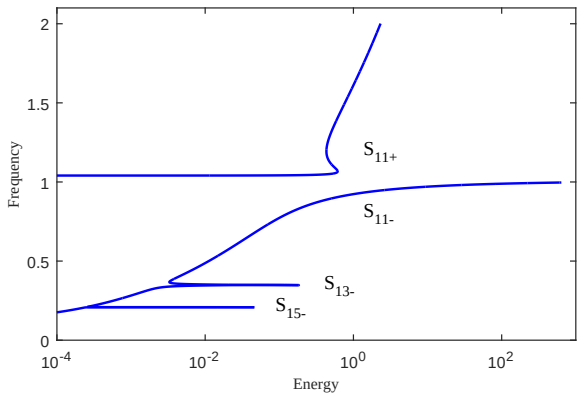

Figure 5. Frequency-Energy Plot of NNMs

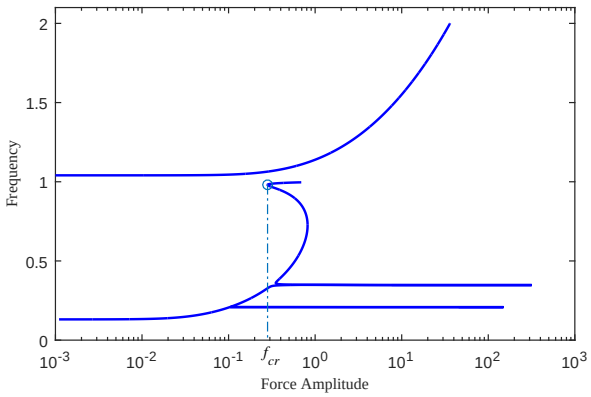

Figure 6. Estimation of Force Amplitude

The outcome of NNM calculations is a Frequency-Energy Plot (FEP) that reveals the evolution of the fundamental frequency of NNM versus the total conserved energy during the periodic motion (see Fig. 5). It can be observed that the FEP is featured by two backbone branches ($S_{11}+$ for in-phase NNM and $S_{11}-$ for out-of-phase NNM) and tongues ($S_{13}-$ and $S_{15}-$) emanating from the backbone. In particular, motion along the $S_{11}-$ branch represents the basic targeted energy transfer mechanism [3]. It relies on the mode localization in NNMs, since NNMs may have their modal shapes varying with the oscillation frequency. As shown in Fig. 7a-c, if the frequency is not close to 1, the motion is always localized to the piezoelectric NES. In weakly damped dynamics, as the damped motion follows branch $S_{11}-$ with decreasing energy, an irreversible energy transfer could accordingly take place from the mechanical structure to the piezoceramics. The tongues $S_{13}-$ and $S_{15}-$ are subharmonic branches that consist of multifrequency periodic solutions. For example, Fig. 7d also depicts period motions on the $S_{13}-$ tongue. The tongues highlight that the NES has no preferential resonant frequency due to the essential nonlinearity. They are capable of engaging in $1:3$ or $1:5$ internal resonance with the mechanical structure. Theoretically it is demonstrated that there generally exist a countable infinite of such internal resonance for nonlinear systems [3, 22]. Fig. 5 only gives the approximation of $1:3$ or $1:5$ internal resonances due to the intrinsic low-pass filtering effect of HBM by setting the retained harmonics $N_h = 5$. Nevertheless, it is sufficient to describe the global trend of backbones.

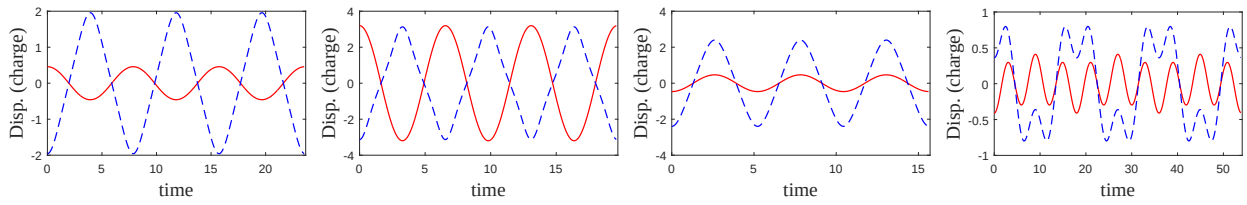

Figure 7. Periodic motions in: (a) S11-, $\omega = 0.8$; (b) S11-, $\omega = 0.96$; (c) S11+, $\omega = 1.2$; (d) S13-, $\omega = 0.35$. (——— x(t); – – – q(t)).

3.3. Correlation between NNMs and nonlinear forced responses

A grasp of NNMs gives insights into the dynamic characteristics of the underlying conservative nonlinear system. In the linear modal analysis framework, structural forced responses can be approximated based on linear normal modes by means of mode superposition. However, NNMs can not be directly used to predict forced responses of the damped nonlinear system in the same way. Correlation between NNMs and nonlinear forced response is explored by following an energy balancing concept initially put forward by Hill *et al* [23] and recently further developed by Kuether *et al* [24]. A fundamental property of NNMs lays the cornerstone of energy balancing: they can be excited when a harmonic forcing cancels the damping force in the nonlinear system. From an energy viewpoint, energy dissipation due to damping force over a periodic motion should equal the energy input from a single-point harmonic forcing $\mathbf{f}(t) = [f_{\text{amp}} \sin \omega t, 0]^{\text{T}}$:

$$\int_0^{2\pi/\omega} \mathbf{y}'(t)^{\text{T}} \mathbf{f}(t) \text{d}t = \int_0^{2\pi/\omega} \mathbf{y}'(t)^{\text{T}} \mathbf{D} \mathbf{y}'(t) \text{d}t \tag{15}$$

With a knowledge of the damping matrix, energy balancing allows to estimate the harmonic forcing amplitude f_{amp} that could excite a NNM $\mathbf{y}(t)$ of the nonlinear system at resonance, as

shown in Fig. 6. One can observe the existence of a force amplitude threshold of $f_{\mathrm{cr}} = 0.28$, below which it implies a single resonance in the vicinity of $\omega = 1$, i.e. the 1st bending mode frequency of the cantilevered beam. On the contrary, above this critical value, multiple resonances might arise and the dynamics of the nonlinear system undergoes essential changes.

Prediction of this critical force amplitude is of practical significance for NES designs. Among the main drawbacks of nonlinear energy sinks in a variety of research efforts are the multiplicity of forced response regimes and energy-dependent performance. For example, the widely reported high isolated response curves (IRCs) are intrinsic limitations for NES acting as nonlinear vibration absorbers [12, 14]. Nevertheless, detecting an IRC outside the continued path is beyond the capability of numerical continuation. Occurrence of undetectable IRCs with high amplitudes is not acceptable for an effective NES design. The energy balancing technique offers a useful tool for avoiding an underestimation of IRCs of high response level. By foreseeing a single resonance for a harmonic forcing below the threshold value, one can ensure the reliability and uniqueness of the main response branch obtained by continuation. It helps to design the nonlinear dynamics such that high isolated response curves can be eliminated in some way.

3.4. Forced vibration of the coupled piezomechanical system

The frequency response function of the vertical displacement at the free end of the beam under a single-point harmonic excitation f_{ext} applied in the middle area (see Fig. 3) is calculated by HBM with $N_h = 3$ harmonics retained. For a purely numerical investigation, an external forcing with constant amplitude will be used. The resultant dimensionless modal force amplitude f_{amp} is 0.181. As declared before, the nonlinear shunt circuit possesses four key parameters $(\varepsilon, \beta, \delta_{\mathrm{res}}, \theta)$. An exhaustive exploration of forced responses in the high dimensional parameter space is a challenge. Next, a strong dependency of forced response regimes on the individual parameters will be shown, respectively.

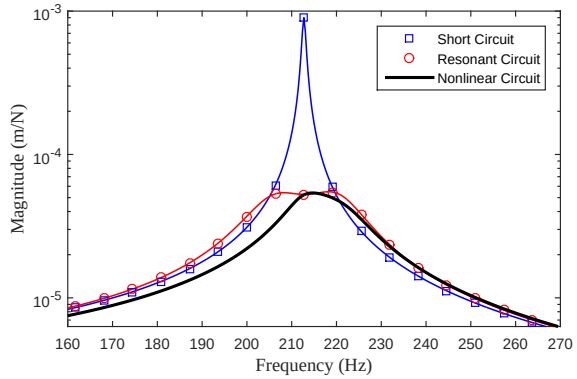

Figure 8. Frequency response function for $(\varepsilon = 0.1, \beta = 1, \delta_{\mathrm{res}} = 0.01, \theta = 0.1)$

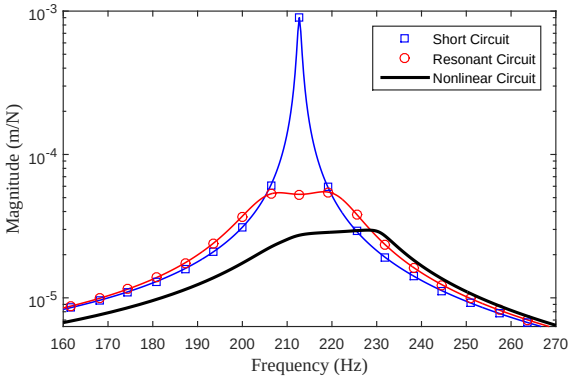

Figure 9. Frequency response function for $(\varepsilon = 0.1, \beta = 0.5, \delta_{\mathrm{res}} = 0.01, \theta = 0.1)$

To start our investigation, Fig. 8 gives a typical frequency response function in physical coordinates with a parameter set $(\varepsilon = 0.1, \beta = 1, \delta_{\mathrm{res}} = 0.01, \theta = 0.1)$ for the nonlinear shunt circuit. Note that the nonlinear shunt parameters are identical with those used for NNM calculations in Fig. 5 and Fig. 6. The dimensionless modal force amplitude f_{amp} is far below the threshold value f_{cr}. Hence, it can be inferred that no isolated response curves exist and therefore the solution branch traced by HBM in conjunction with continuation gives reliable predictions of forced responses. They have also been confirmed in time-history simulations. The performance of the well-tuned resonant shunt circuit and nonlinear shunt circuit are compared in Fig. 8. "Short circuit" denotes the response curve of the beam with electrodes of piezoceramics

in short circuit. It appears that the nonlinear shunt circuit performs nearly as well as the tuned resonant circuit in terms of vibration reduction. However, with a small inductance requirement of $\varepsilon = 0.1$, the nonlinear circuit outperforms the linear resonant circuit.

The impacts of variations of the damping parameter β and nonlinear coefficient θ on forced responses are now examined. The linear term δ_{res} remains invariable since essential nonlinearity characterizes the nonlinear shunt circuit constructed in the framework of NES theory. A decreasing damping parameter $\beta = 0.5$ significantly improves the damping performance of the nonlinear shunt circuit, as shown in Fig. 9. While an increasing nonlinear coefficient $\theta = 0.2$ induces drastic changes in forced responses in Fig. 10. Apparently, the nonlinearly shunted piezoceramics fail to perform as an effective vibration absorber in this case.

We continue our investigation with an increasing inductance value, i.e. $(\varepsilon = 0.3, \beta = 1, \delta_{\text{res}} = 0.01, \theta = 0.1)$. By monitoring Floquet multipliers, two Neimark-Sacker (NS) bifurcation points are observed in the nonlinear frequency response curves (see Fig. 11). At these bifurcation points, the branch of periodic solutions loses its stability and evolves into a branch of quasi-periodic solutions, although the system is single-frequency excited. This phenomenon is in agreement with the literatures, where quasi-periodic response regimes are extensively reported and experimentally evidenced [14, 25, 26]. Quasi-periodic responses are predicted by a so-called variable coefficient harmonic balance method developed in our previous research effort [27].

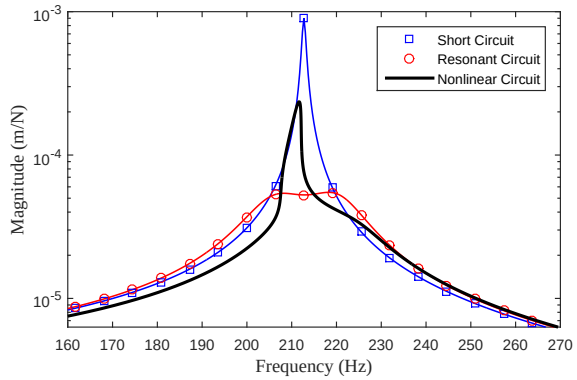

Figure 10. Frequency response function for $(\varepsilon = 0.1, \beta = 1, \delta_{\text{res}} = 0.01, \theta = 0.2)$

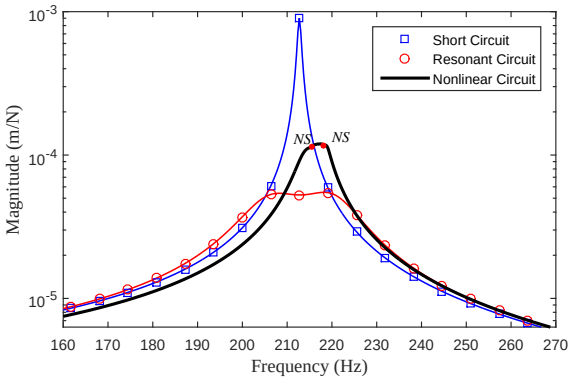

Figure 11. Frequency response function for $(\varepsilon = 0.3, \beta = 1, \delta_{\text{res}} = 0.01, \theta = 0.1)$

It should be pointed out that the topological structures of NNMs for systems presented in Fig. 10 and Fig. 11 are supposed to be different from the backbone curves in Fig. 5, as well as the resultant force amplitude threshold. Accordingly, the possibility of detached response curves could not be excluded. In brief summary, the configuration of nonlinear shunt circuit in Fig. 8 gives acceptable and efficient performance in terms of vibration mitigation. Since the nonlinearly shunted piezoceramics are explored as vibration absorbers, their effective bandwidth will be examined subsequently.

3.5. Robustness of nonlinear shunt circuit

Aiming at examining the effective bandwidth of the nonlinear shunt circuit, this section is to unveil the forced responses of the global piezo-mechanical system in case of variations in structural properties. To this end, the cantilevered beam is assumed to undergo a slight change by the addition of a modified mass weighted 0.035 Kg (see Fig. 4). The modified piezo-mechanical system experiences approximately 5% frequency drift for the 1$^{\text{st}}$ bending mode, as summarized in Table 3. Performances of both the resonant circuit and nonlinear circuit with fixed electrical parameters, are then revaluated and compared, as shown by dashed lines in Fig. 12.

Table 3. Parameters of the modified system for 1st bending mode.

Description	Value	Description	Value
EMCC. $K(\%)$	9.02	Natural Freq. ω_{sc}	202.22 Hz
Coupling term κ	0.0459	Natural Freq. ω_{iso}	203.07 Hz

Fig. 12 clearly illustrates an appealing feature of the nonlinear shunt circuit, i.e. nonexistence of a preferential resonance frequency. Correct tuning according to the structural frequency is vital for a resonant circuit. The detuned resonant circuit loses its desired damping effectiveness around the altered structural frequency of the modified system. On the contrary, the nonlinear response curve globally shifts to the left-hand side. Furthermore, the damping performance of the nonlinear shunt circuit seems to improve slightly in terms of vibrational amplitude reduction. According to the NES theory, this phenomenon is attributed to the capability of NES to resonantly interact with modes of the primary system at arbitrary frequency ranges. A robust damping performance is therefore expected to withstand the evolving structural properties. It results in a broad frequency bandwidth of the nonlinearly shunted piezoceramics performing as a vibration absorber.

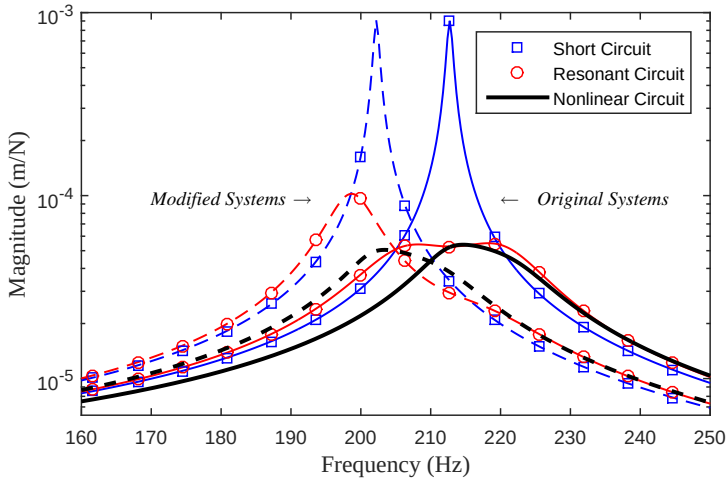

Figure 12. Performances of resonant/nonlinear circuit integrated into different beams. solid lines: original systems; dashed lines: modified systems

4. Conclusion

This research aims to numerically confirm the feasibility of exploring nonlinearly shunted piezoceramic materials as effective vibration absorbers in the framework of NES theory.

A nonlinearly shunted piezoelectric vibration absorber is built and applied in a cantilevered beam. Intensional introduction of essential nonlinearity into the conventional resonant circuits characterizes this piezoelectric vibration absorber. However, it also gives rise to complex dynamics for the integrated piezo-mechanical system under harmonic excitation. The energy balancing technique is employed to gap the bridge between undamped nonlinear normal modes and forced responses of the nonlinear system. Prediction of a harmonic forcing amplitude

threshold raises the possibility of designing an effective NES device exempted from high amplitude detached response curves.

A rough parameter study suggests an efficient configuration of the nonlinear shunt circuit. It enables the nonlinearly shunted piezoceramics to work effectively and robustly in a broad frequency band in terms of vibration mitigation. Above all, this paper provides a preliminary numerical studies in depth for a nonlinearly shunted piezoelectric vibration absorber. It is supposed to pave the way for experimental investigations that are currently in process.

Acknowledgments

The support of the National Natural Science Foundation of China (Grant No. 51405460), the Collaborative Innovation Center of Advanced Aero-Engine are gratefully acknowledged.

References

[1] Hagood N W and von Flotow A 1991 *Journal of Sound and Vibration* **146** 243–268
[2] Viguie R, Kerschen G and Ruzzene M 2009 *Proc. SPIE, Active and Passive Smart Structures and Integrated Systems* vol 7288 (San Diego, California, USA) pp 72882B–72882B
[3] Vakakis A and Gendelman O 2009 *Nonlinear Targeted Energy Transfer in Mechanical and Structural Systems* (Springer)
[4] McFarland D M, Bergman L A and Vakakis A F 2005 *International Journal of Non-Linear Mechanics* **40** 891–899
[5] Bellet R, Cochelin B, Herzog P and Mattei P O 2010 *Journal of Sound and Vibration* **329** 2768–2791
[6] Al-Shudeifat M A, Wierschem N, Quinn D D, Vakakis A F, Bergman L A and Spencer Jr B F 2013 *International Journal of Non-Linear Mechanics* **52** 96–109
[7] Wang J, Wierschem N, J S, F B and Lu X 2015 *Engineering Structures* **94** 9–15
[8] Luo J, Wierschem N and Fahnestock L 2014 *Journal of Engineering Mechanics* **140** 04014009
[9] Luo J, Wierschem N E and Hubbard S A 2014 *Engineering Structures* **77** 34–48
[10] Lee Y S, Kerschen G, McFarland D M, Vakakis A F, Bergman L A and Wouw N v d 2007 *AIAA journal* **45** 2391–2400
[11] Zhou B, Thouverez F and Lenoir D 2014 *Journal of Sound and Vibration* **333** 2520–2542
[12] Alexander N A and Schilder F 2009 *Journal of Sound and Vibration* **319** 445–462
[13] Detroux T, Habib G, Masset L and Kerschen G 2015 *Mechanical Systems and Signal Processing* **60C61** 799–809
[14] Gourc E, Michon G, Seguy S and Berlioz A 2014 *Journal of Vibration and Acoustics* **136** 021021–021021
[15] Neubauer M and Wallaschek J 2013 *Mechanical Systems and Signal Processing* **36** 36–52
[16] Chevallier G, Ghorbel S and Benjeddou A 2008 *Smart Materials and Structures* **17** 065007
[17] Gluskin E E 1999 *Journal of The Franklin Institute* **336** 1035–1047
[18] Groll G and Ewins D 2001 *Journal of Sound and Vibration* **241** 223–233
[19] Grolet A and Thouverez F 2012 *Mechanical Systems and Signal Processing* **30** 43–60
[20] Seydel R 1995 *Practical bifurcation and stability analysis : from Equilibrium to chaos* (New York: Springer)
[21] Nayfeh A H and Balachandran B 1995 *Applied nonlinear dynamics : analytical, computational, and experimental methods* (New York: Wiley)
[22] Renson L, Kerschen G and Cochelin B 2016 *Journal of Sound and Vibration* **364** 177–206
[23] Hill T, Cammarano A, Neild S and Wagg D 2014 *Proceedings of EURODYN 2014* 1981–1988
[24] Kuether R J, Renson L, Detroux T, Grappasonni C, Kerschen G and Allen M S 2015 *Journal of Sound and Vibration* **351** 299–310
[25] Starosvetsky Y and Gendelman O V 2008 *Journal of Sound and Vibration* **315** 746–765
[26] Starosvetsky Y and Gendelman O 2008 *Nonlinear Dynamics* **51** 47–57
[27] Zhou B, Thouverez F and Lenoir D 2015 *Mechanical Systems and Signal Processing* **64C65** 233–244